Int. J. Heat Mass Transfer. Vol. 22, pp. 705–719

0017–9310/79/0501-0705 $02.00/0

HEATED TURBULENT FLOW OF HELIUM–ARGON MIXTURES IN TUBES*

P. E. PICKETT, M. F. TAYLOR and D. M. MCELIGOT
Aerospace and Mechanical Engineering Department, The University of Arizona, Tucson, AZ 85721, U.S.A.

(*Received* 17 *May* 1977 *and in revised form* 13 *September* 1978)

Abstract—The results of a numerical and experimental investigation of friction and heat-transfer parameters for turbulent flow of helium–argon mixtures in smooth, electrically heated, vertical circular tubes are presented. Mixtures with molecular weights between 15.3 and 29.7 are used; these values correspond to molecular Prandtl numbers between 0.42 and 0.49. Inlet Reynolds numbers range from 31 200 to 102 000, maximum wall temperatures from 392 to 828 K, maximum wall-to-bulk temperature ratios to 1.82, and pressures from 4.7 to 9.7 atm. Popular existing experimental correlations, developed using gases with Prandtl numbers of the order of 0.7, are found to overpredict the observed Nusselt numbers. By comparison of numerical calculations and measured constant property Nusselt numbers, turbulent Prandtl numbers are determined in the wall region. The validity of using these deduced turbulent Prandtl numbers is examined for conditions where the properties vary significantly.

NOMENCLATURE

a, exponent used to account for temperature variation of viscosity;
A_{cs}, cross-sectional area of tube;
b, exponent used to account for temperature variation of thermal conductivity;
c, velocity of sound;
c_p, specific heat at constant pressure;
D, inside diameter;
g, gravitational constant;
g_c, dimensional conversion factor;
G, average mass flux, $\dot{m}/A_{cs}$;
h, heat-transfer coefficient;
i, specific enthalpy;
k, thermal conductivity;
l, mixing length;
$\dot{m}$, mass flow rate;
$\bar{M}$, molal mass;
p, pressure;
q'', heat flux;
r, radius;
R, gas constant for a particular gas;
$\mathscr{R}$, universal gas constant;
T, temperature;
u, velocity in axial direction;
v, velocity in radial direction;
x, axial distance from start of heating;
y, radial distance from wall.

Greek symbols

ε/κ, force constant in Lennard-Jones potential;
ε_h, eddy diffusivity for heat;
ε_m, eddy diffusivity for momentum;
γ, ratio of specific heats, c_p/c_v;
κ, empirical constant in van Driest mixing length model, 0.4;
μ, absolute viscosity;
ν, kinematic viscosity;
ρ, density;
σ, force constant in Lennard-Jones potential;
τ, shear stress.

Non-dimensional parameters

f, friction factor, $2g_c\rho\tau_w/G^2$;
Gr, Grashof number based on wall heat flux, $gD^4q_w''/(\nu^2\mu c_pT)_i$;
Nu, Nusselt number, hD/k;
$\bar{p}$, pressure drop, $\rho_i g_c(p_i-p)/G^2$;
Pr, Prandtl number, $c_p\mu/k$; Pr_t, turbulent Prandtl number;
q^+, heat flux parameter, $q_w''/(Gc_{p,i}T_i)$;
$\bar{r}$, radial distance, r/r_w;
Re, Reynolds number, GD/μ;
$\bar{x}$, axial distance, x/D;
y^+, wall distance parameter, $y(g_c\tau_w/\rho)^{1/2}/\nu$;
y_l^+, empirical constant in van Driest mixing length model, 26.

Subscripts

av, lengthwise average;
b, evaluated at bulk temperature;
cp, constant property condition;
DB, Dittus–Boelter;
DKM, Drew, Koo and McAdams;
eff, effective;
i, inlet; an index;
Max, maximum;
ref, reference;
t, turbulent;
vD, van Driest;
w, wall.

*This work was performed under the auspices of the Office of Naval Research.

1. INTRODUCTION

THE CLOSED cycle gas turbine system, or closed Brayton cycle, has been found to be an efficient, compact and versatile system for propulsion and power plant applications [1, 2]. The gas entering the compressor is not restricted to air at atmospheric conditions. The entire cycle can be pressurized to reduce the size of components and alternate gases can be employed to avoid contamination and corrosion problems. In addition to being chemically inert, several of the noble gases have higher molecular weights than air; in conjunction with their higher specific heat ratios, higher aerodynamic efficiencies and improved heat-transfer result. Based on thermodynamic cycle studies Bammert and Klein [3] concluded that considerable savings in the cost of a gas turbine cycle could be obtained by mixing a heavier gas with helium.

In preliminary design studies for application of inert gas mixtures to closed gas turbine systems, Vanco [4] compared the expected heat-transfer coefficients of the mixtures for turbulent flow in ducts using a version of the Colburn analogy [5] which may be written as:

$$Nu = 0.023Re^{0.8}Pr^{1/3}. \tag{1}$$

This relationship is supposedly valid for the range $0.5 < Pr < 100$, but is primarily based on experiments for fluids with $Pr \approx 0.7$ or greater. For gases, with $Pr \approx 0.7$, McAdams [6] recommended the Dittus–Boelter correlation with the coefficient modified,

$$Nu_{DB} = 0.021Re^{0.8}Pr^{0.4}, \tag{2}$$

instead. The difference is about 10% for most gases (with $Pr \approx 0.7$). As shown later the Prandtl number for a mixture of helium and argon can be of the order of 0.4; no data are available for this range so it is important to test the validity of these correlations. This testing is one of the purposes of the present experiment.

For predictions of heat transfer to turbulent flows many engineering analyses employ the turbulent Prandtl number, $Pr_t = \varepsilon_m/\varepsilon_h$, to estimate effective thermal conductivity from correlations for momentum transfer. As shown in surveys by Blom [7], Quarmby and Quirk [8] and Reynolds [9], there still exists considerable uncertainty concerning the proper variation of Pr_t with molecular Prandtl number. At $Pr \approx 0.7$, some idealized analyses suggest that $Pr_t > 1$ while others yield $Pr_t < 1$. A second purpose of the present work is to determine whether Pr_t differs significantly from unity at $Pr \approx 0.4$–0.5 in the wall region, which dominates the convective heat-transfer behavior.

The next section summarizes pertinent knowledge of the transport properties of mixtures of helium and argon. Section 3 briefly describes the numerical analysis to be employed and, for fully established conditions, presents the predicted Nusselt numbers, which disagree with correlations (1) and (2) when Reynolds analogy ($Pr_t = 1$) is employed. The experiment is then described. In Section 5 the data are extrapolated to the constant property idealization to test the correlations and then the diagnostic technique of McEligot *et al.* [10] is applied to estimate $Pr_{t,w}$. The following section extends the data to heating rates where the temperature dependence of the transport properties becomes significant and demonstrates that numerical predictions based on the value of Pr_t deduced from measurements at low heating rate are still adequate. Major conclusions are reiterated in the last section.

2. TRANSPORT PROPERTIES OF HELIUM–ARGON MIXTURES

The properties needed for this study were compressibility, viscosity, thermal conductivity, specific heat, enthalpy, speed of sound and the gas constant. The properties of air have been studied extensively; for the comparison data the NBS tables of Hilsenrath *et al.* [11] were used in this investigation. The properties of helium and helium–argon mixtures were calculated theoretically. For all gases the viscosity and thermal conductivity were assumed to be independent of pressure.

The helium and helium–argon mixtures were assumed to be ideal gases, thus making the compressibility equal to unity. This assumption is reasonable for the range of pressures (100–970 kPa) and temperatures (290–830 K) used in this experiment. Since helium and argon are monatomic and the temperature range in this study was not too large, the relation [12]

$$c_p = (5/2)R = (5/2)\mathscr{R}/\tilde{M} \tag{3}$$

was used to calculate the specific heat.

Using the ideal gas and constant specific heat assumptions, one may derive simple equations for the enthalpy and speed of sound [13]:

$$i = c_p(T - T_{ref})$$

and

$$c = (\gamma RT)^{1/2} = [(5/3)RT]^{1/2}. \tag{4}$$

The Lennard–Jones [6–12] potential can be employed in the Chapman–Enskog kinetic theory to predict thermal conductivity, viscosity and Prandtl number of binary mixtures of inert gases [14]. There has been considerable experimental study of the pure gases but few data exist on the mixtures.

With force constants, ε/κ and σ, as suggested by Hirschfelder *et al.* [14] the predicted viscosity for helium falls about 8% below the data of Dawe and Smith [15] and Kalelkar and Kestin [16] at temperatures around 900°C. Likewise, the predicted thermal conductivity is about 9% lower than the measurements of Saxena and Saxena [17] up to 1100°C. Similar discrepancies exist for argon. Using force constants suggested by DiPippo and Kestin [18] instead leads to essential agreement with the values recommended by the Thermophysical Properties Research Center [19].

The mixture properties are shown in Fig. 1. The solid curves were calculated with the force constants recommended by DiPippo and Kestin: $\sigma = 2.158$A and $\varepsilon/\kappa = 86.2$ K for helium and $\sigma = 3.292$A and $\varepsilon/\kappa = 152.75$ K for argon. The dashed curves compare values calculated from the recommendations of Hirschfelder *et al.*

The viscosity of the mixture varies only slightly with molecular weight (composition). From pure helium to pure argon the variation is only about 15%; for mole fractions of argon greater than 0.25 the viscosity is almost constant. As with pure gases the viscosity increases with temperature. The predicted values agree well with the data of Tanzler [19] at 75 atm and of Kalelkar and Kestin [16].

The mixture thermal conductivity decreases by a factor of five or more as the molecular weight increases from pure helium to pure argon and it increases with temperature. Agreement with the data of Gambhir and Saxena [20] and of Cheung *et al.* [21] is close. The measurements of Paterson *et al.* [22] at 50 atm show that neglect of pressure variation is justified. It appears that the higher temperature data of Mason and von Ubisch [23] refute the model; however, in a critical review Gandhi and Saxena [24] have observed that the measurements of von Ubisch appear to be systematically higher than others they reviewed.

In a companion study for laminar flow, McEligot *et al.* [25] demonstrated that the temperature dependence of the viscosity and thermal conductivity could be approximated as

$$\frac{\mu}{\mu_{\text{ref}}} = \left(\frac{T}{T_{\text{ref}}}\right)^a \text{ and } \frac{k}{k_{\text{ref}}} = \left(\frac{T}{T_{\text{ref}}}\right)^b. \tag{5}$$

The exponent a ranges from 0.7 to 0.8 and b falls between about 0.7 and 0.75.

As a consequence of the variation of thermal conductivity and specific heat vs molecular weight the Prandtl number decreases to a minimum of about 0.42 at $\tilde{M} \approx 16$ from about 2/3 for the pure gases. It is about 0.48 at the molecular weight of air. The temperature dependence is almost negligible since the power law exponents for μ and k differ so little.

In the present study the calculated properties were applied in tabular form in the data reduction programs. For numerical analyses, correlations of the calculated values—such as equations (5)—were used to reduce computation time.

3. NUMERICAL ANALYSIS

In this paper, analysis is by the numerical method of Bankston and McEligot [26] utilizing finite control volume approximations to solve the governing equations,

Continuity:

$$\frac{\partial \hat{\rho}\hat{u}}{\partial \bar{x}} + \frac{2}{\bar{r}}\frac{\partial \hat{\rho}\hat{v}}{\partial \bar{r}} = 0. \tag{6a}$$

x-Momentum:

$$\hat{\rho}\hat{u}\frac{\partial \hat{u}}{\partial \bar{x}} + 2\hat{\rho}\hat{v}\frac{\partial \hat{u}}{\partial \bar{r}} = \frac{\mathrm{d}\bar{p}}{\mathrm{d}\bar{x}} + \frac{4}{Re_i}\frac{1}{\bar{r}}\frac{\partial}{\partial \bar{r}}\left(\bar{r}\hat{\mu}_{\text{eff}}\frac{\partial \hat{u}}{\partial \bar{r}}\right). \tag{6b}$$

Energy:

$$\hat{\rho}\hat{u}\frac{\partial \hat{i}}{\partial \bar{x}} + 2\hat{\rho}\hat{v}\frac{\partial \hat{i}}{\partial \bar{r}} = \frac{4}{Re_i Pr_i}\frac{1}{\bar{r}}\frac{\partial}{\partial \bar{r}}\left(\bar{r}\frac{\hat{k}_{\text{eff}}}{\hat{c}_p}\frac{\partial \hat{i}}{\partial \bar{r}}\right). \tag{6c}$$

Integral continuity:

$$\int_0^1 \hat{\rho}\hat{u}\bar{r}\,\mathrm{d}\bar{r} = \tfrac{1}{2}. \tag{6d}$$

Idealizations implied by these forms are (a) the axisymmetric boundary-layer approximations, (b) steady flow at low velocities, (c) constant mixture concentration, and (d) negligible axial conduction. The circumflex (ˆ) represents non-dimensionalization with respect to the value of the quantity at the entrance with the exception of $\hat{u}$ and $\hat{v}$ which are normalized by the inlet bulk velocity.

Gas properties may be idealized as

$$\hat{\rho} = \hat{p}/\hat{T};\ \hat{\mu} = \hat{T}^a;\ \hat{k} = \hat{T}^b;\ \hat{c}_p = \hat{T}^d. \tag{7}$$

Initial conditions are specified and boundary conditions are the no-slip, impermeable wall with the observed wall heat flux variation specified.

The effective viscosity is predicted with a combination of the van Driest mixing length [27] and Reichardt middle law [28],

$$l_{vD} = \kappa y[1 - \exp(-y^+/y_l^+)] \tag{8a}$$

and

$$\varepsilon_m = \varepsilon_{vD}\cdot\left(2 - \frac{y}{r_w}\right)\cdot\left[1 + 2\left(\frac{r}{r_w}\right)^2\right]\Big/6. \tag{8b}$$

The wall temperature is used to evaluate properties in y^+. With $\kappa = 0.4$ and $y_l^+ = 26$, this representation yields adiabatic friction factors within about 1% of the Drew *et al.* correlation [29] over the range $3 \times 10 < Re < 3 \times 10^5$. This van Driest model has also been found to be most successful in predicting wall temperatures in conditions where strong heating rates cause significant gas property variation [26].

The program uses implicit algebraic equations to represent the governing equations. These equations are iterated at each axial step to treat their coupling and the non-linear terms. Mesh spacing is chosen to provide Nusselt numbers and friction factors within about 2% of their converged values. The node nearest the wall falls at $y^+ \approx 0.5$ or less.

For predictions under the constant property idealizations the exponents a, b and d are set to zero and $\hat{\rho}$ is taken as unity. Then if the inlet condition is a fully developed flow, only the energy equation is solved.

Heat-transfer results for fully established conditions with constant properties are shown in Fig. 2. Reynolds analogy, $Pr_t = 1$, has been assumed here. Normalization by the Dittus–Boelter correlation (2) is chosen due to its popularity in representing heat transfer to gases (with 0.021 as the coefficient); this

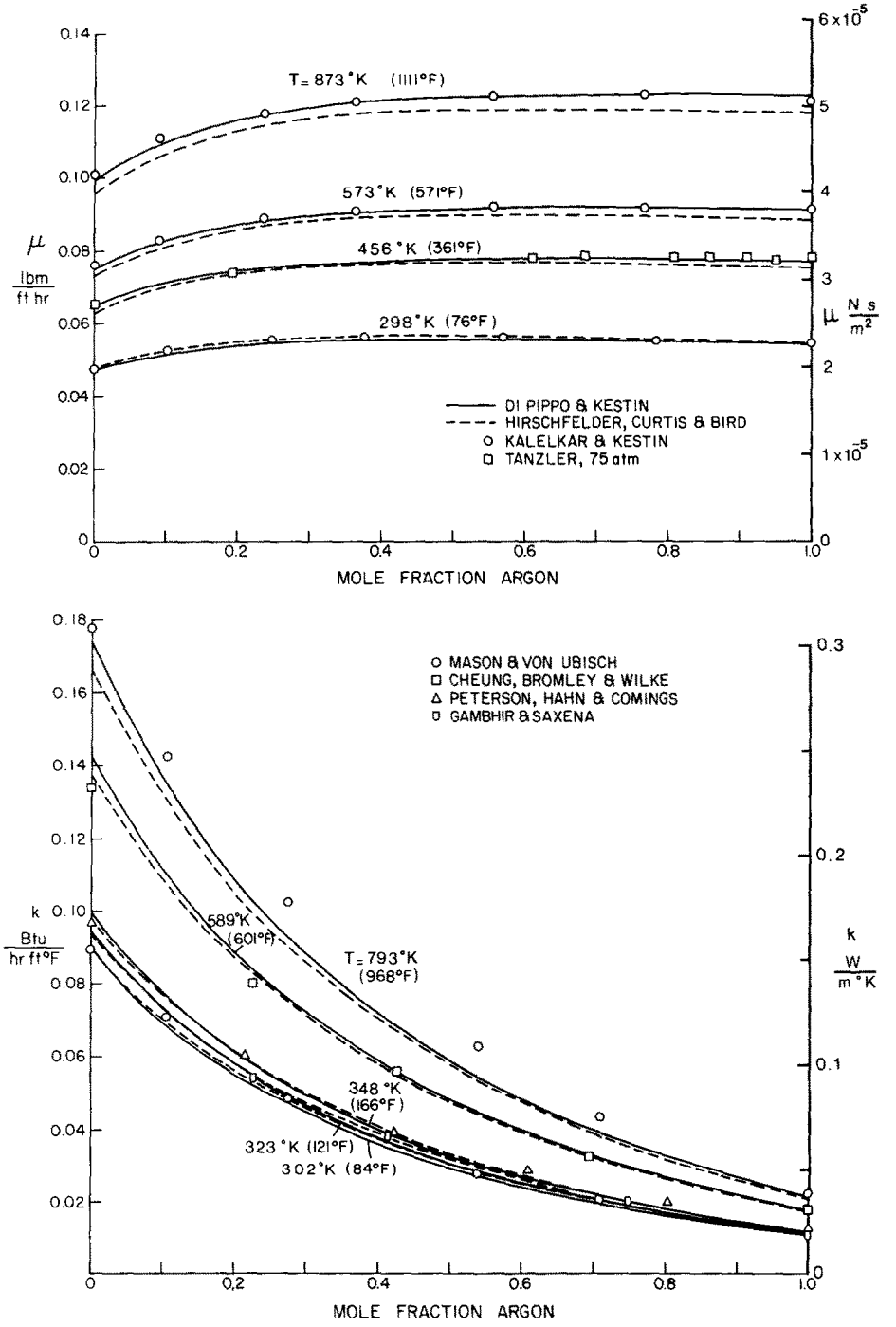

FIG. 1. Transport properties of helium–argon mixtures. Pressure = 1 atm unless noted.

correlation is often taken as a reference in representing effects of gas property variation. It describes gas data for low heating rates well over the range $2400 < Re < 2 \times 10^5$ [51, 52].

The present predictions diverge from correlations (1) and (2) as the Prandtl number is reduced and the Reynolds number is increased. If the present results are reasonable, the two correlations would overpredict the Nusselt number with the Colburn analogy, used by Vanco [4], being about 15% worse than the Dittus–Boelter correlation for helium–argon mixtures. Whether Reynolds analogy and these numerical predictions are adequate must be determined by experiment.

4. EXPERIMENT

The experimental apparatus, arrangement, and procedure were similar to those used by Campbell and Perkins [30]. Instead of a square duct, a circular tube of Hastelloy-X was used as the test section. This vertical tube had an inside diameter of 0.312 cm

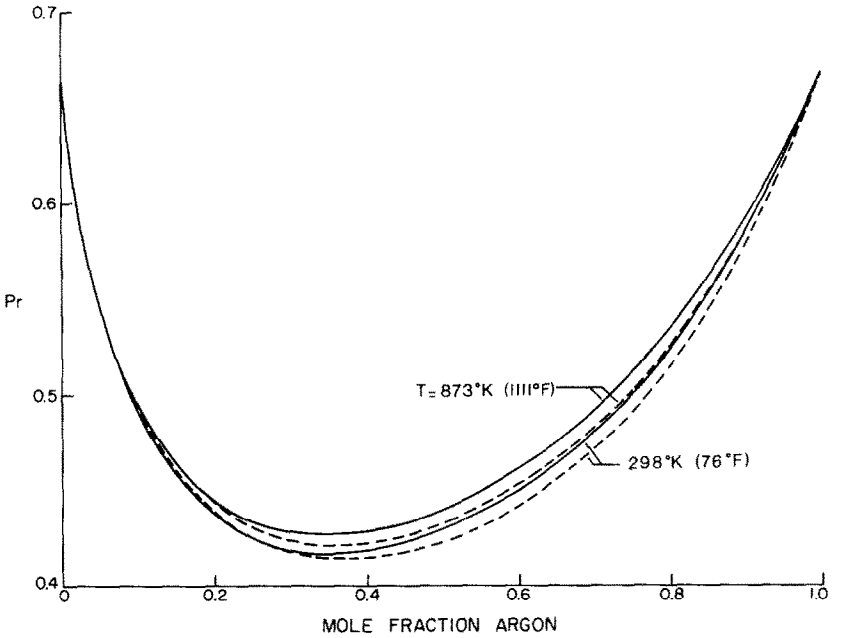

FIG. 1. Transport properties of helium–argon mixtures. Pressure = 1 atm unless noted.

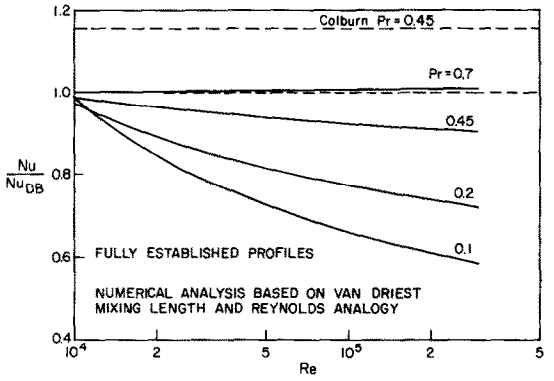

FIG. 2. Heat-transfer predictions for fully established conditions. Constant fluid properties.

(1/8 in) and a wall thickness of 0.056 cm (0.022 in). The test section consisted of a heated section 98 diameters in length preceded by an unheated section 92 diameters in length. The unheated section ensured that the flow approached a fully developed profile prior to heating. Electrical resistance heating of the test section yielded an axial heat flux distribution which exponentially approached a constant value within three diameters and then remained constant within a few per cent. As in the work of Campbell and Perkins the test section itself served as the electrical resistance heater; thin stainless steel electrodes were brazed to the tube and AC current from a line voltage stabilizer was supplied via variable transformers. Two pressure taps were used. One was located in the lower electrode and the other eight diameters below the upper electrode.

Sixteen premium grade Chromel–Alumel thermocouples, 0.013 cm (0.005 in) diameter, were spot welded to the heated section of the tube using the parallel junction suggested by Moen [31]. Thermocouple conduction error was calculated from the heat loss calibration data and a relation developed by Hess [32]; the thermocouple conductance was estimated from the emissivity of the bare wires and a natural convection correlation for small Rayleigh numbers. The correction is of the order ot 1% of the difference between the tube temperature and the environmental temperature; at $Re \approx 3 \times 10^4$, the effects are approximately $1\frac{1}{2}$–2% on the Nusselt number and 3–4% on the deduced turbulent Prandtl number.

With the exception of air, the gas was supplied in commercial gas cylinders. The manufacturer, Matheson Gas Products Division, provided the mixtures to our specifications in lots of four bottles. For the first two batches concentration was determined locally by gas chromotography; due to equipment difficulties, concentration measurements on samples of the same mixture varied by 2% on a volume basis so adiabatic friction factor measurements were used to confirm the concentration as reported by the manufacturer. For the last two batches Matheson determined the concentration with a thermal conductivity column with sample variation to within 0.8 and 0.4% (however, the experimental uncertainty of the technique is estimated as 2%); these concentrations were also confirmed by the adiabatic friction data.

To measure the higher flow rates, our positive displacement meter was replaced by a Meriam laminar flow element. The latter was calibrated to measure the flow rate within $\pm 1.5\%$. Heise gages, inclined water manometers, and vertical mercury or water manometers were used to measure static pressure and pressure drop.

Table 1. Range of variables in the present experiment

	Air	Helium	Helium–argon
Experimental runs	25	4	28
Molecular weight	28.97	4.003	15.3–29.7
Inlet bulk Reynolds number	32 900–100 000	30 200	31 200–102 000
Exit bulk Reynolds number	19 900–89 000	18 400–26 600	17 000–68 000
Inlet bulk Prandtl number	0.719	0.667	0.419–0.486
Exit bulk Prandtl number	0.682	0.667	0.426–0.495
Maximum T_w/T_b	1.90	1.75	1.82
Maximum T_w (K)	817	789	828
Maximum q^+	0.0027	0.0027	0.0032
Maximum Gr/Re_i^2	8.90×10^{-5}	4.84×10^{-5}	3.22×10^{-3}
Maximum Mach number	0.26	0.25	0.33
x/D for local bulk Nusselt numbers	2.1–82.1	2.1–82.1	2.1–82.1

Table 2. Data for helium–argon mixture with molal mass = 29.70

x/D	T_w [°K]	T_w/T_b	q''_w [Kw/m²]	$Re_{bx} \times 10^{-4}$	Nu_{bx}
Run 102H, $q^+(41) = 0.002579$, $Pr_i = 0.486$, $M_i = 0.268$, $\bar{p}(90.4) = 2.45$, $\dot{m} = 16.5$ kg/h, $T_i = 295$ K, $p_i = 8.19$ atm					
2.1	494.3	1.656	305.6	8.069	149.6
4.1	531.8	1.747	312.4	7.931	129.6
8.1	574.0	1.815	314.4	7.680	111.7
16.4	624.2	1.832	316.1	7.218	96.5
24.6	659.1	1.807	316.5	6.829	88.5
32.5	686.8	1.770	316.9	6.500	83.4
40.9	711.4	1.723	316.7	6.192	79.9
48.9	736.1	1.687	316.8	5.932	76.6
57.0	757.4	1.646	316.4	5.696	74.4
65.0	772.8	1.599	316.5	5.489	74.1
73.4	794.2	1.565	315.9	5.292	72.4
81.6	807.6	1.520	314.9	5.119	72.8
90.4	811.0	1.458	304.5	4.952	74.4
Run 103H, $q^+(41) = 0.002044$, $Pr_i = 0.486$, $M_i = 0.173$, $\bar{p}(90.3) = 2.12$, $\dot{m} = 16.4$ kg/h, $T_i = 295$ K, $p_i = 8.15$ atm					
2.1	452.5	1.521	242.4	8.052	150.7
4.1	484.8	1.604	245.9	7.942	128.0
8.1	512.7	1.646	248.4	7.739	114.6
16.4	547.8	1.655	249.5	7.359	102.0
24.5	574.8	1.642	249.8	7.029	94.5
32.4	594.8	1.614	250.2	6.743	90.6
40.8	616.3	1.588	250.0	6.470	86.5
48.8	634.7	1.561	250.3	6.236	83.9
56.9	652.8	1.534	250.0	6.020	81.6
64.9	667.0	1.502	250.1	5.826	80.9
73.3	682.1	1.472	249.8	5.640	80.1
81.5	696.1	1.443	249.1	5.474	79.8
90.3	699.5	1.393	241.7	5.314	82.0

Table 2. *—continued*

x/D	T_w [°K]	T_w/T_b	q''_w [Kw/m²]	$Re_{bx} \times 10^{-4}$	Nu_{bx}
Run 104H, $q^+(41) = 0.001192$, $Pr_i = 0.486$, $M_i = 0.173$, $\bar{p}(90.1) = 1.62$, $\dot{m} = 16.4$ kg/h, $T_i = 296$ K, $p_i = 8.16$ atm					
2.1	387.5	1.309	142.2	8.099	151.8
4.1	402.5	1.347	144.8	8.034	135.1
8.1	418.8	1.377	145.6	7.912	121.0
16.4	438.6	1.390	146.0	7.672	109.9
24.5	453.1	1.387	146.2	7.454	104.3
32.4	463.5	1.374	146.4	7.258	102.4
40.8	477.2	1.368	146.2	7.062	98.2
48.7	489.4	1.361	146.3	6.888	95.2
56.8	499.7	1.348	146.3	6.723	93.8
64.8	508.7	1.333	146.4	6.571	93.4
73.1	519.9	1.323	146.1	6.420	91.6
81.3	528.9	1.309	145.8	6.283	91.3
90.1	531.2	1.278	142.5	6.145	95.2
Run 105H, $q^+(41) = 0.000653$, $Pr_i = 0.486$, $M_i = 0.173$, $\bar{p}(90.0) = 1.30$, $\dot{m} = 16.5$ kg/h, $T_i = 296$ K, $p_i = 8.19$ atm					
2.1	345.2	1.173	79.1	8.154	155.7
4.1	353.9	1.196	79.4	8.118	135.6
8.1	360.9	1.208	80.0	8.049	126.5
16.4	370.9	1.216	80.1	7.911	117.6
24.5	378.8	1.218	80.2	7.780	112.7
32.4	385.1	1.215	80.2	7.660	110.8
40.7	392.6	1.215	80.1	7.536	107.2
48.7	398.8	1.212	80.2	7.423	105.5
56.8	405.1	1.209	80.1	7.313	103.8
64.7	410.1	1.202	80.2	7.209	104.1
73.1	416.8	1.200	80.0	7.103	102.0
81.2	421.6	1.193	79.9	7.005	102.7
90.0	422.6	1.175	78.5	6.904	109.0
Run 107H, $q^+(41) = 0.003165$, $Pr_i = 0.486$, $M_i = 0.083$, $\bar{p}(90.4) = 2.97$, $\dot{m} = 6.3$ kg/h, $T_i = 296$ K, $p_i = 6.6$ atm					
2.1	483.9	1.594	142.3	3.044	74.0
4.1	532.3	1.711	148.7	2.980	61.8
8.1	584.2	1.792	150.3	2.864	51.6
16.4	641.4	1.795	150.9	2.657	43.9
24.6	679.9	1.753	150.5	2.488	40.1
32.5	709.3	1.699	150.2	2.348	37.9
40.9	734.7	1.636	149.5	2.221	36.6
48.9	757.6	1.582	149.1	2.116	35.7
57.0	780.4	1.533	148.2	2.022	34.9
65.0	799.2	1.484	147.6	1.940	34.8
73.4	819.4	1.439	146.7	1.862	34.7
81.6	835.1	1.394	145.1	1.795	35.2
90.4	838.5	1.331	134.3	1.733	35.7

Table 1 summarizes the range of variables covered in this investigation. The significant raw data, control parameters and deduced local Nusselt and Reynolds numbers for the helium–argon experiments are presented in Tables 2 and 3. A more detailed discussion of the experiment and more complete tabulations of the data are available in a report* by Pickett [33].

*This report will be available from the Defense Documentation Center in the United States.

Table 2.—*continued*

x/D	T_w [°K]	T_w/T_b	q''_w [Kw/m²]	$Re_{bx} \times 10^{-4}$	Nu_{bx}
Run 108H, $q^+(41) = 0.002210$, $Pr_i = 0.486$, $M_i = 0.083$, $\bar{p}(90.2) = 2.39$, $\dot{m} = 6.4$ kg/h, $T_i = 296$ K, $p_i = 6.6$ atm					
2.1	425.6	1.413	99.8	3.078	75.7
4.1	455.8	1.487	103.6	3.033	64.5
8.1	485.8	1.534	104.9	2.949	56.3
16.4	522.7	1.544	105.2	2.792	49.2
24.5	548.2	1.524	105.2	2.657	45.9
32.4	570.0	1.499	105.1	2.541	43.7
40.8	588.6	1.464	104.8	2.431	42.6
48.8	608.6	1.439	104.6	2.338	41.1
56.9	623.7	1.405	104.3	2.252	40.9
64.9	639.4	1.376	104.1	2.176	40.7
73.3	657.4	1.352	103.3	2.103	39.9
81.4	669.7	1.321	102.7	2.038	40.6
90.2	675.9	1.279	95.3	1.977	40.5
Run 109H, $q^+(41) = 0.001414$, $Pr_i = 0.486$, $M_i = 0.083$, $\bar{p}(90.1) = 1.91$, $\dot{m} = 6.3$ kg/h, $T_i = 297$ K, $p_i = 6.6$ atm					
2.1	378.2	1.262	64.0	3.087	77.3
4.1	395.4	1.305	66.4	3.058	67.6
8.1	414.7	1.340	66.9	3.002	58.8
16.4	435.2	1.346	67.2	2.895	53.7
24.5	450.4	1.337	67.2	2.798	51.3
32.4	465.2	1.329	67.1	2.712	49.1
40.8	476.6	1.309	67.0	2.628	48.7
48.7	490.6	1.300	66.9	2.553	47.0
56.8	501.3	1.283	66.7	2.484	46.9
64.8	511.3	1.265	66.7	2.420	47.1
73.1	523.3	1.252	66.4	2.358	46.6
81.3	533.7	1.237	65.9	2.301	46.5
90.1	535.7	1.203	62.2	2.245	48.7
Run 111H, $q^+(41) = 0.000898$, $Pr_i = 0.486$, $M_i = 0.084$, $\bar{p}(90.0) = 1.58$, $\dot{m} = 6.4$ kg/h, $T_i = 293$ K, $p_i = 6.6$ atm					
2.1	344.4	1.170	40.6	3.191	78.4
4.1	355.4	1.199	42.5	3.172	69.2
8.1	367.7	1.223	42.8	3.135	60.5
16.4	381.8	1.234	42.9	3.060	54.9
24.5	391.8	1.233	42.9	2.992	52.6
32.4	400.8	1.229	42.9	2.929	51.0
40.7	409.3	1.223	42.8	2.866	50.1
48.7	417.8	1.218	42.7	2.808	49.0
56.8	426.1	1.212	42.6	2.754	48.1
64.7	432.9	1.203	42.6	2.702	48.2
73.1	441.3	1.198	42.4	2.651	47.3
81.2	448.9	1.191	42.1	2.604	46.7
90.0	451.5	1.171	39.9	2.557	47.7
Run 112H, $q^+(41) = 0.000574$, $Pr_i = 0.486$, $M_i = 0.084$, $\bar{p}(90.0) = 1.40$, $\dot{m} = 6.4$ kg/h, $T_i = 293$ K, $p_i = 6.6$ atm					
2.1	327.6	1.114	26.1	3.188	75.8
4.1	334.7	1.133	27.1	3.176	66.5
8.1	341.1	1.144	27.4	3.152	61.2
16.4	350.4	1.154	27.4	3.103	55.4
24.5	356.9	1.155	27.4	3.057	53.3
32.3	362.3	1.153	27.4	3.014	52.5
40.7	368.1	1.151	27.3	2.970	51.5
48.7	373.2	1.147	27.3	2.930	51.1
56.8	379.4	1.148	27.2	2.890	49.4
64.7	383.6	1.142	27.2	2.853	49.9
73.0	388.9	1.139	27.1	2.815	49.5
81.2	394.4	1.137	26.9	2.779	48.4
89.9	396.4	1.125	25.7	2.743	49.4

Table 3. Data for helium–argon mixture with molal mass = 15.30

x/D	T_w [°K]	T_w/T_b	q''_w [Kw/m²]	$Re_{bx} \times 10^{-4}$	Nu_{bx}
Run 124H, $q^+(41) = 0.000563$, $Pr_i = 0.419$, $M_i = 0.113$, $\bar{p}(90.0) = 1.40$, $\dot{m} = 6.4$ kg/h, $T_i = 295$ K, $p_i = 6.9$ atm					
2.1	326.9	1.108	51.4	3.210	70.7
4.1	333.3	1.125	52.3	3.198	61.6
8.1	339.9	1.137	52.6	3.176	55.4
16.4	348.5	1.145	52.6	3.130	50.8
24.5	355.1	1.146	52.6	3.087	48.7
32.3	360.7	1.145	52.6	3.047	47.7
40.7	366.4	1.144	52.6	3.005	46.8
48.7	372.0	1.143	52.6	2.967	45.9
56.8	377.7	1.142	52.5	2.929	45.0
64.7	382.7	1.139	52.5	2.894	44.7
73.0	388.4	1.137	52.4	2.858	43.8
81.2	393.2	1.134	52.2	2.824	43.8
89.9	395.5	1.122	51.1	2.789	45.8
Run 125H, $q^+(41) = 0.001360$, $Pr_i = 0.419$, $M_i = 0.113$, $\bar{p}(90.1) = 1.87$, $\dot{m} = 6.4$ kg/h, $T_i = 295$ K, $p_i = 6.9$ atm					
2.1	372.7	1.253	123.2	3.178	70.2
4.1	388.4	1.292	125.6	3.150	60.7
8.1	405.2	1.320	126.3	3.098	53.7
16.4	426.3	1.332	126.6	2.996	48.3
24.5	441.8	1.327	126.7	2.904	45.8
32.4	454.7	1.316	126.8	2.822	44.5
40.8	467.9	1.305	126.7	2.741	43.3
48.7	480.8	1.295	126.8	2.669	42.2
56.8	493.6	1.285	126.6	2.601	41.2
64.8	504.6	1.272	126.7	2.538	40.9
73.1	517.1	1.261	126.4	2.477	40.3
81.3	528.5	1.250	126.1	2.420	39.8
90.1	534.5	1.225	122.5	2.364	40.9
Run 126H, $q^+(41) = 0.000551$, $Pr_i = 0.419$, $M_i = 0.234$, $\bar{p}(90.0) = 1.42$, $\dot{m} = 11.1$ kg/h, $T_i = 296$ K, $p_i = 5.7$ atm					
2.1	332.2	1.139	87.5	5.583	102.7
4.1	337.8	1.153	88.4	5.563	92.6
8.1	344.2	1.165	88.7	5.526	84.4
16.4	352.6	1.174	88.8	5.451	78.1
24.5	359.1	1.176	88.8	5.380	75.1
32.3	364.4	1.175	88.9	5.313	73.8
40.7	369.9	1.174	88.8	5.246	72.5
48.7	375.6	1.174	88.9	5.184	70.9
56.8	381.1	1.174	88.8	5.122	69.6
64.7	385.9	1.171	88.8	5.064	69.3
73.0	391.1	1.170	88.8	5.005	68.6
81.2	395.9	1.167	88.6	4.950	68.3
89.9	397.1	1.153	87.6	4.893	73.0
Run 127H, $q^+(41) = 0.002156$, $Pr_i = 0.419$, $M_i = 0.112$, $\bar{p}(90.2) = 2.36$, $\dot{m} = 6.4$ kg/h, $T_i = 296$ K, $p_i = 6.9$ atm					
2.1	416.8	1.385	194.7	3.132	71.1
4.1	441.6	1.443	198.4	3.089	61.1
8.1	468.8	1.484	199.6	3.009	53.2
16.4	502.7	1.492	200.3	2.861	47.0
24.5	527.5	1.476	200.6	2.733	44.0
32.4	547.6	1.451	200.8	2.621	42.3
40.8	566.9	1.423	200.7	2.515	41.2
48.8	585.6	1.399	201.0	2.424	40.2
56.9	610.9	1.391	200.4	2.338	37.7
64.9	628.0	1.367	200.5	2.263	37.2
73.2	645.3	1.344	200.1	2.191	36.9
81.4	661.7	1.321	199.4	2.126	36.7
90.2	669.2	1.281	192.7	2.063	37.9

Table 3.—*continued*

x/D	T_w [°K]	T_w/T_b	q''_w [Kw/m²]	Ra_{bx} $\times 10^{-4}$	Nu_{bx}
Run 128H, $q^+(41) = 0.003037$, $Pr_i = 0.419$, $M_i = 0.113$, $\bar{p}(90.4) = 2.90$, $\dot{m} = 6.4$ kg/h, $T_i = 297$ K, $p_i = 6.9$ atm					
2.1	475.2	1.564	274.5	3.110	67.1
4.1	516.1	1.659	279.8	3.050	56.2
8.1	560.1	1.723	282.1	2.943	47.8
16.4	615.3	1.735	283.4	2.748	40.7
24.6	654.0	1.704	283.7	2.588	37.1
32.5	683.9	1.660	283.9	2.453	35.2
40.9	712.1	1.611	283.6	2.327	33.6
48.9	737.4	1.567	283.6	2.223	32.6
57.0	761.8	1.525	283.1	2.129	31.8
65.0	781.1	1.480	282.7	2.047	31.8
73.4	794.6	1.425	282.9	1.969	32.8
81.6	825.8	1.408	280.5	1.897	31.1
90.4	831.8	1.349	269.9	1.833	32.4
Run 129H, $q^+(41) = 0.001254$, $Pr_i = 0.419$, $M_i = 0.233$, $\bar{p}(90.1) = 1.94$, $\dot{m} = 11.1$ kg/h, $T_i = 297$ K, $p_i = 5.7$ atm					
2.1	382.8	1.295	198.2	5.483	101.3
4.1	397.8	1.333	200.3	5.440	88.8
8.1	413.8	1.361	201.1	5.358	79.4
16.4	434.4	1.376	201.7	5.199	71.7
24.5	449.6	1.375	201.9	5.055	67.9
32.4	462.1	1.367	202.2	4.926	65.9
40.8	474.7	1.358	202.2	4.798	64.1
48.7	487.1	1.350	202.4	4.684	62.4
56.8	498.8	1.342	202.4	4.577	61.1
64.8	509.1	1.331	202.5	4.477	60.5
73.1	520.3	1.321	202.4	4.380	59.7
81.3	530.8	1.311	202.1	4.291	59.2
90.1	533.5	1.281	199.0	4.202	62.5
Run 130H, $q^+(41) = 0.001919$, $Pr_i = 0.419$, $M_i = 0.186$, $\bar{p}(90.2) = 2.22$, $\dot{m} = 11.0$ kg/h, $T_i = 298$ K, $p_i = 7.1$ atm					
2.1	429.3	1.432	301.0	5.394	99.8
4.1	453.2	1.489	304.7	5.328	86.7
8.1	479.1	1.530	306.3	5.207	76.5
16.4	512.0	1.545	307.5	4.977	67.8
24.5	535.7	1.534	308.1	4.777	63.4
32.4	555.1	1.514	308.6	4.601	60.8
40.8	574.4	1.491	308.7	4.432	58.7
48.8	592.9	1.472	309.1	4.286	56.7
56.9	609.8	1.450	309.1	4.150	55.5
64.9	623.7	1.424	309.4	4.025	55.2
73.2	641.1	1.405	309.2	3.906	54.1
81.4	654.3	1.381	308.8	3.800	54.2
90.2	659.2	1.338	302.9	3.695	56.6
Run 131H, $q^+(41) = 0.002791$, $Pr_i = 0.419$, $M_i = 0.186$, $\bar{p}(90.4) = 2.80$, $\dot{m} = 11.0$ kg/h, $T_i = 298$ K, $p_i = 7.1$ atm					
2.1	489.6	1.618	435.2	5.340	98.7
4.1	527.7	1.707	441.0	5.247	84.1
8.1	568.7	1.767	444.0	5.078	72.8
16.4	631.4	1.783	446.4	4.770	62.5
24.6	658.7	1.758	447.4	4.511	57.3
32.5	688.6	1.722	448.2	4.293	54.0
40.9	716.3	1.678	448.5	4.089	51.6
48.9	741.8	1.640	449.0	3.915	49.7
57.0	765.3	1.601	448.9	3.760	48.4
65.0	783.4	1.556	449.1	3.624	48.2
73.4	804.7	1.519	449.0	3.495	47.6
81.6	823.0	1.482	447.9	3.380	47.6
90.4	827.3	1.421	437.7	3.265	49.6

The experimental uncertainties were estimated by the method of Kline and McClintock [34]. Typical values for the Nusselt number are 13% at $x/D \approx 1.2$ decreasing to 4% at $x/D \approx 25$ for low heating rates and slightly less for the higher heating rates. The dominant uncertainty is in the bulk stagnation temperature which depends on the mass flow rate, electrical power and the heat loss calibration.

The test section was a bare tube surrounded by a draft shield so heat loss was by radiation and natural convection. The heat loss was calibrated as a function of axial position and temperature from measurements without internal flow. During runs with flow the fraction of power dissipated to the environment, instead of to the internal gas flow, increases with axial position and temperature level and decreases with Reynolds number. For the helium–argon data the worst situation in the present data occurred at $Re_i \approx 3.1 \times 10^4$ and $\tilde{M} = 29.7$ where q''_{loss}/q''_w reached 0.15 at the highest heating rate; thus, for this condition a 10% uncertainty in heat loss would cause less than 2% uncertainty in the heat flux to the gas. For mixtures with lower molecular weights, improved convective heat transfer led to lower heat loss ratios, e.g. $(q''_{loss}/q''_w) \approx 0.07$ with $\tilde{M} = 15.3$ at the same conditions.

Adiabatic friction factors were measured before each series of heated runs. These results were used as a check of the measurements of pressure, mixture molecular weight, and flow rate. The measured friction factors were compared to the experimental correlation of Drew *et al.* [29],

$$f_{DKM} = 0.0014 + 0.125 Re^{-0.32}. \quad (9)$$

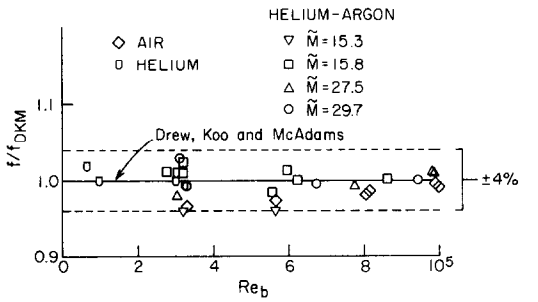

FIG. 3. Comparison of adiabatic friction factors to Drew *et al.* correlations for air, helium and helium–argon mixtures.

Figure 3 shows the measured friction factors plotted as a function of Reynolds number. Air and helium data points are included for comparison. All the measured values are within 4% of correlation (9), and three-quarters are within 2%. The data for the mixture with $\tilde{M} = 15.83$ and for helium show the best agreement. No systematic variation with molecular weight seems evident.

5. HEAT TRANSFER WITH CONSTANT PROPERTIES

In order to deduce the turbulent Prandtl number without complications introduced by its possible variation with heating rate, the measurements were

extrapolated to the constant property idealization by the approach of Malina and Sparrow [35]. For this method, a series of experimental runs are taken with the same inlet Reynolds number and gas composition but with successively higher heating rates. At each thermocouple location the measured Nusselt numbers are plotted vs the local temperature difference, $T_w - T_b$. An extrapolation to $T_w - T_b = 0$ yields the deduced Nusselt number for constant property conditions, Nu_{cp}. A comparable extrapolation of the experimental uncertainty provides an estimate of the validity of these data. For the range of data reported the uncertainty in constant properties Nusselt number varied from 9% at small axial distances to about 5% at large distances.

For fully developed conditions with air or helium as the fluid, the ratio Nu_{cp}/Nu_{DB} varied from 0.94 to 1.0 without any evident dependence on Reynolds number. With helium–argon mixtures of Prandtl number 0.42–0.49 the ratio varied from 0.83 to 0.93. This reduction in the normalized value corresponds to the trend predicted in Fig. 2. Since the reduction is greater than predicted by the analysis, it is a first indication that a turbulent Prandtl number greater than unity may be appropriate for the mixtures.

In addition to equations (1) and (2), several other correlations have been recommended for heat transfer to gases with fully established temperature profiles downstream in tubes. Kays [36] recommends the relation

$$Nu = 0.022 Re^{0.8} Pr^{0.6} \tag{10}$$

for the range $0.5 < Pr < 1.0$ for the thermal boundary condition of a constant wall heat flux. This analytical correlation agreed with the present mixture data within 6% so it can be considered valid to $Pr = 0.42$; at $Pr \approx 0.7$ it shows slightly better agreement than the Dittus–Boelter correlation (2).

Sleicher and Rouse [37] suggest a correlation for the ranges $0.1 < Pr < 10^5$ and $10^4 < Re < 10^6$,

$$Nu_b = 5 + 0.015 Re_f^m Pr_w^n \tag{11}$$

where

$$m = 0.88 - 0.24/(4 + Pr_w)$$

and

$$n = (1/3) + 0.5 \exp(0.6 Pr_w).$$

The subscripts, b, f and w, refer to evaluation of properties at bulk, film and wall temperatures, respectively, when property variation is significant. For constant properties in the range of the present data this relation predicts lower values than the simpler correlation of Kays. At $Pr \approx 0.7$ the predictions of Sleicher and Rouse correspond to the lower limit of the data and at $Pr \approx 0.45$ they are a few per cent below the lower limit of these data. While the magnitudes differ from the data slightly, their trend with Prandtl number corresponds to the present predictions and measurements.

In order to deduce the turbulent Prandtl number the technique of McEligot *et al.* [10] is applied. Essentially, hypothesized distributions $Pr_t(y)$ are introduced in the numerical analysis and the predicted Nusselt numbers, $Nu(x)$, are compared to the data, $Nu_{cp}(x)$. Variations in the shape of $Pr_t(y)$ are reflected in variation in the shape of $Nu(x)$ in the thermal entry region. One of the main advantages of this matching technique is that it concentrates on determining Pr_t accurately in the region which is most important for predicting surface temperatures in flows heated from the wall.

Application of the technique requires accurate velocity and eddy diffusivity profiles $u^+(y^+)$ and $\varepsilon(y^+)/\nu$. In the present study these are generated from the van Driest mixing length model modified by the Reichardt "middle law", equations (8). Although the van Driest model currently seems quite successful and has been used widely for calculation of the wall region of turbulent flows [40, 41] there is reason to question its detailed behavior in the viscous layer, $y^+ \lesssim 30$. Sleicher [42] and Coles [43] presented tentative profiles obtained by synthesis of data taken with hot wires and pitot tubes during the late 1940's and 1950's; the resulting eddy diffusivities are 10–20% greater than deduced from the van Driest model in the range $10 \leqslant y^+ \leqslant 30$. As pointed out by Lykoudis in discussion of Sleicher's report, the values of ε/ν derived from velocity profile measurements can be highly uncertain. Plots of $u^+(y^+)$ are sensitive to the determination of τ_w since it appears in the denominator of u^+ and the numerator of y^+. Further, near the wall the per cent uncertainty in Δy can be substantial when using $\Delta u/\Delta y$ to calculate ε, particularly since $\tau_t \ll \tau$ for $y^+ < 10$. More recently, Andersen *et al.* [44] obtained careful hot wire data for $y^+ \gtrsim 3$; the difference from the van Driest profile is about 10% near $y^+ = 10$ but the uncertainty $\delta u/u$ is of the same order [45]. Further from the wall, at $y^+ \approx 29$ the uncertainties in u^+ and y^+ are in the range of 3–5% due to the uncertainty in τ_w. For the outer wall of an annulus Heikal and Hatton [46] show very close agreement with the van Driest prediction in the range $11 < y^+ < 30$ but do not include estimated experimental uncertainties. In summary, it appears that a definitive mean velocity profile has not yet been determined for the viscous layer; thus, it is best to consider the present results for Pr_t to be dependent on the assumption of the van Driest model for the viscous layer.

In this study, as in the demonstration in [10], the experimental uncertainty at small axial distances was too large to determine $\mathrm{d}Pr_t/\mathrm{d}(y/r_w)$ clearly. Consequently, a constant value of Pr_t was used in the present calculations; the sensitivity tests in reference [10] showed that it is essentially equivalent to an effective $Pr_{t,w}$ for the wall region. Only results for x/D greater than eight were used to determine $Pr_{t,w}$.

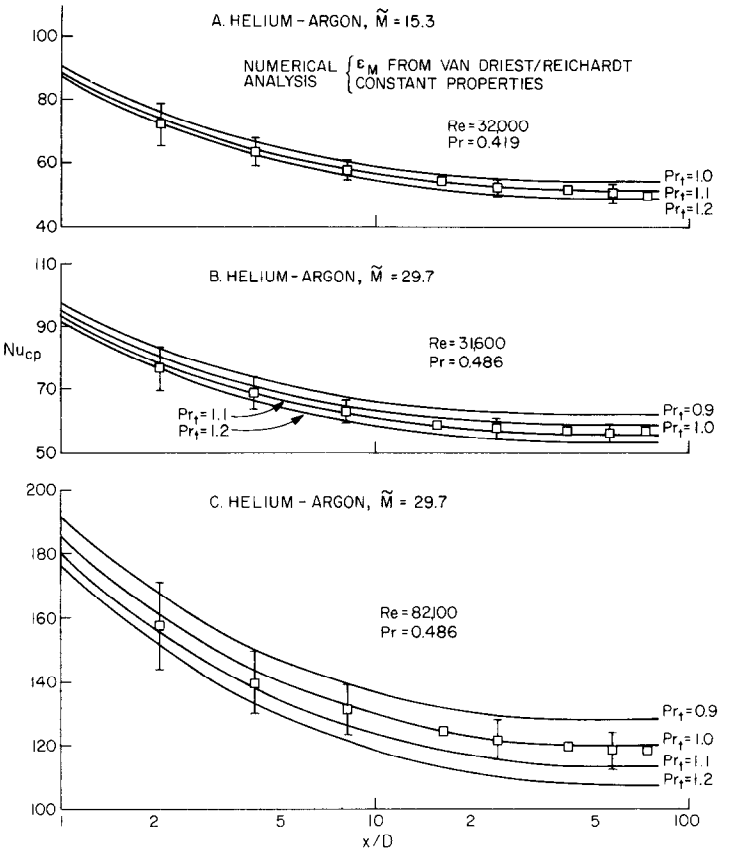

FIG. 4. Examples of the comparisons between measured $Nu_{cp}(x)$ and predicted $Nu(x)$ as used to deduce Pr_{tw} for constant properties.

Figure 4 illustrates examples of the comparisons between measured $Nu_{cp}(x)$ and predicted $Nu(x)$ used to determine $Pr_{t,w}$. Examples for three Reynolds numbers and two Prandtl numbers are shown. Brackets indicating the estimated experimental uncertainties of the $Nu_{cp}(x)$ are also included.

Figure 4(a) shows the measured and calculated Nu_{cp} for a helium–argon mixture with a molecular weight of 15.3, Prandtl number of 0.42, and Reynolds number of 32 000. The turbulent Prandtl number is seen to be about 1.1 or slightly less. From comparisons on similar graphs, $Pr_{t,w}$ was estimated to be 1.1 ± 0.1 for helium–argon mixtures with molecular weights of approximately 15, Prandtl numbers of 0.42, and Reynolds numbers between 32 000 and 55 200. Measurements and predictions are shown in Figs. 4(b) and (c) for a helium–argon mixture at a molecular weight of 29, Prandtl number of 0.486, and Reynolds numbers of 31 600 and 82 100. From similar graphs, $Pr_{t,w}$ was estimated to be 1.0 ± 0.1 for the range of helium–argon mixtures with molecular weights between 27 and 30, Prandtl numbers between 0.46 and 0.49, and Reynolds numbers between 31 600 and 102 000.

The effect of Reynolds number on $Pr_{t,w}$ can be examined qualitatively using the results in Figs. 4(b) and (c), but the experimental uncertainty prohibits a quantitative determination. These results are for the same Prandtl number ($Pr = 0.486$), but two different Reynolds numbers: 31 600 and 82 100. For x/D greater than eight, and at the lower Reynolds number, the measured $Nu_{cp}(x)$ data are slightly below the calculated $Nu(x)$ curve for a $Pr_{t,w}$ of 1.0. At the higher Reynolds number and same axial locations, the measured $Nu_{cp}(x)$ are slightly above the prediction for $Pr_{t,w} = 1.0$. For the stated conditions, it appears that $Pr_{t,w}$ may have a weak dependence on Reynolds number, and may decrease slightly as the Reynolds number increases.

The effect of molecular Prandtl number on turbulent Prandtl number can be examined using the observations from Figs. 4(a) and (c) which are summarized in Table 4. The air data of McEligot *et al.* [10] can also be considered since the present study shows $Pr_{t,w}$ to vary only slightly with Reynolds number. For the range shown in Table 4, $0.42 \gtrsim Pr < 0.7$, the turbulent Prandtl number increases as the molecular Prandtl number decreases as suggested by the review of Reynolds [9].* However, reference to Fig. 4 shows that predictions based on O. Reynolds' analogy are still valid to within 5–10% which is adequate for many engineering applications.

*This observation must be tempered by the recent data of Serksnis *et al.* [47] for hydrogen–carbon dioxide mixtures at $Pr \approx 1/3$; a range $0.95 \gtrsim Pr_t \gtrsim 1$ is determined by the present method.

Table 4. Variation of $Pr_{t,w}$ with respect to molecular Prandtl number

Gas	Molecular weight	Prandtl number	$Pr_{t,w}$	Reynolds number
Helium–argon	15.3	0.419	1.1 ± 0.1	32000
Helium–argon	29.7	0.486	1.0 ± 0.1	31600
Air [10]	28.97	0.72	0.9 ± 0.1	44500

Na and Habib [48] extended an unsteady sublayer treatment of Cebeci [49] and have predicted $Pr_t(y^+)$ over a wide range of molecular Prandtl number. They too predict an increase in Pr_t as Pr decreases and as $y^+ \to 0$. However, examination of their Fig. 8 shows that they predict $1.3 \gtrsim Pr_t \gtrsim 1.5$ in the viscous layer for the range of the present experiments. The results of the present measurements disagree with these values. The present authors suspect that the difficulty lies in the empirical determination of adjustable constants by Na and Habib; for the range $0.02 < Pr < 0.7$ they apparently employed old liquid metal data—often highly uncertain—and some old gas data from experiments with high heating rates.

6. HEATING WITH PROPERTY VARIATION

In order to increase power densities or lower the weight of closed Brayton cycle systems, moderately high heating rates must be employed. Consequently, the temperature-dependence of the fluid transport properties causes significant variation in properties appearing in the coefficients of equations (6) and coupling of the equations. The results and correlations based on the constant properties idealizations become invalid. In this section the modifications accounting for property variation are examined and the application of the turbulent Prandtl number, determined above for constant properties, is tested.

Since only two pressure taps were attached to the test section, local friction factors could not be determined. Overall average friction factors with heat addition were compared to the correlation proposed by Taylor [38]

$$f_{av} = (0.0014 + 0.125 Re_w^{-0.32}) \times (T_{w,av}/T_{b,av})^{-0.5} \quad (12)$$

for the data of a wide variety of experiments with gas flow. Most previous measurements agreed within 10%. For evaluation of this expression, arithmetic averages of the conditions at the two pressure taps were used to calculate the average temperatures and pressure and, hence, density and viscosity. The overall friction factor was determined from the frictional pressure drop,

$$\Delta p_{fr} = p_1 - p_2 - \frac{G^2 R}{g_c}\left(\frac{T_{b2}}{p_2} - \frac{T_{b1}}{p_1}\right)$$

and the modified wall Reynolds number was defined as

$$Re_w = (GD/\mu_w)(T_{b,av}/T_{w,av}).$$

In the present study correlation (12) predicted most of the data within 4%; all are within 10%. These measurements are presented in Fig. 5. Comparison to Fig. 3—which uses the constant properties limit of the same equation—shows a general increase in the normalized data with heating. This increase indicates the exponent on the temperature ratio may be slightly too large, leading to an underprediction of the average wall friction. The effect appears to be most significant for the lower molecular weight mixtures in low Reynolds number flow.

The downstream measurements of the local Nusselt number were compared to correlation (11) of Sleicher and Rouse [37]. Though intended to account for property variation, the values predicted were 15–40% lower than the measurements for the mixtures. Thus, this correlation could yield excessively conservative estimates of surface temperatures in design calculations. Sleicher and Rouse present another correlation to account for the effect

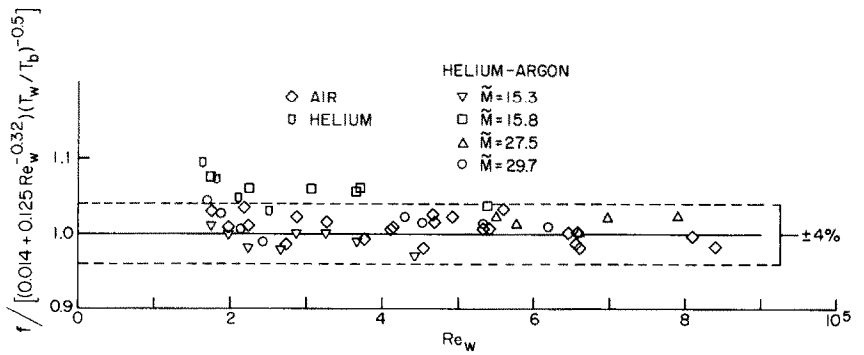

FIG. 5. Comparison of average friction factors to Taylor variable properties correlation for air, helium and helium–argon mixtures.

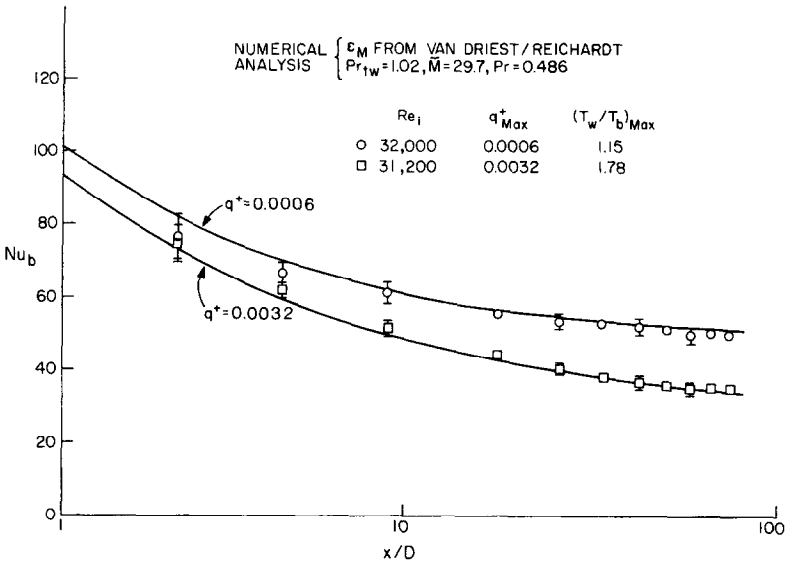

FIG. 6. Comparison of data to numerical predictions accounting for transport property variation.

of gas property variation, their equation (12),

$$Nu_b = 5 + 0.012 Re_b^{0.83}(Pr + 0.29)(T_w/T_b)^q$$

where $q = -\log_{10}(T_w/T_b)^{1/4} + 0.3$ for $x/D > 40$. This equation was not compared to the present data initially since $0.6 < Pr < 0.9$ was listed as its range of validity. More recently it has been verified to within 10% for the downstream data of Tables 2 and 3, with the exception of a few points in two runs, despite the lower Prandtl number.

Magee [39] has suggested accounting for property variation and thermal entry development by applying a multiplicative factor to the constant property correlation. In the range, $2.1 < x/D < 81.6$, his correlation predicted 97% of our data for heat transfer to air and helium to within 10%. Since the transport properties of helium–argon mixtures vary with temperature in approximately the same manner as for air and helium, the same exponent was taken for the temperature ratio. Kays [36] discusses the effect of Prandtl number variation on the thermal entry behavior for circular tubes. As the Prandtl number decreases the thermal entry region is expected to become more pronounced, so a larger coefficient is appropriate for the axial development term. These considerations plus a correlation of the constant properties results [33] lead to

$$Nu_b = 0.021 Re_b^{0.8} Pr_b^{0.55} \times [(T_w/T_b)^{-0.4} + 0.85D/x] \quad (13)$$

which predicts 92% of the present helium–argon data to within 10% for the range $2.1 < x/D < 81.6$. The greatest discrepancy occurs in the range $4 \leqslant x/D \leqslant 16$ at high heating rates; in this situation the measurements are underpredicted by 5–15% [33].

The validity of the deduced values of the turbulent Prandtl number were tested for the conditions of two experimental runs, one with slight property variation and the other with strong heating. Both runs were with the same mixture with $\tilde{M} = 29.7$ and $Pr \approx 0.49$ and essentially the same inlet Reynolds number. For predictions the measured wall heat flux distribution was used for the thermal boundary condition and exponents in equations (5) were taken as $a = 0.772$ and $b = 0.741$ to account for property variation. From the constant property results the turbulent Prandtl number was taken as 1.02.

Comparisons between the two heating rates and the numerical predictions are presented as Fig. 6. These demonstrate that the combined effect of the strong heating rate and the property variation is a reduction in Nu_b of about 1/3 in the downstream region. The difference in Nu decreases as the thermal entry is approached while the temperature ratio peaks near 10–15 diameters, the region where correlation (13) shows the greatest discrepancy.

The numerical predictions and data agree well for both heating rates. This observation is to be expected for the lower heating rate, $q^+ = 0.0006$, since the maximum difference between wall and bulk properties was about 11%. Thus, the conditions did not differ substantially from the constant properties idealization under which the turbulent Prandtl number was deduced.

At the higher heating rate, $q^+ = 0.0032$, the property variation at a cross section approaches 60%. Thus, it is reasonable to ask whether the heating causes a significant effect on the turbulent Prandtl number in the important wall region. Apparently, it does not. Applying the value deduced for constant properties leads to close agreement between predicted and measured Nusselt numbers at this heating rate as well (Fig. 6). While not an exhaustive examination, this test is an initial indication that Pr_t is not a strong function of heating rate. One plausible physical explanation is presented by Serksnis *et al.* [47]: Reynolds analogy corresponds

to an impulsive transport model and, since flow visualization [50] shows the majority of the turbulent momentum transport to occur via the abrupt phases of motion in the viscous layer, one would expect the turbulent energy transport in the region to be impulsive. Property variation due to increased heating rates likely modifies the dominant scales and frequencies but not the basic phenomenon itself.

Extension to other molecular Prandtl numbers, Reynolds numbers and heating rates is the subject of further work now in progress.

7. CONCLUSIONS

From experiments and numerical analyses for the heated flow of helium–argon mixtures with molecular Prandtl numbers in the range 0.42 to 0.49, the following major conclusions may be drawn. The Dittus–Boelter correlation and Colburn analogy, based on measurements for $Pr \gtrsim 0.7$, overpredict Nusselt numbers for fully developed flow with constant properties in this range. Equation (12) of Sleicher and Rouse predicts most of the downstream data of Tables 2 and 3 within 10%. For the range $2.1 < x/D < 82$ correlation (13) of the present work represents the local Nusselt numbers well.

With the van Driest/Reichardt model (equations 8) taken as a basis for predicting momentum transfer, the turbulent Prandtl number in the wall region was deduced to be 1.1 ± 0.1 for $Pr \approx 0.42$ and 1.0 ± 0.1 for $Pr \approx 0.49$ for constant properties; variation with Reynolds number was slight. These results do not differ substantially from Reynolds analogy. At $Re_i \approx 3 \times 10^4$ and $Pr = 0.49$, the value of Pr_{tw} deduced in low heating rate experiments provides adequate predictions when property variation becomes significant.

Acknowledgements—The study reported herein has been supported by the Office of Naval Research under Contract N00014-75-C-0694. Calculations were conducted on the CDC 6400 of the University of Arizona Computer Center. We appreciate the help of Dr. Wm. G. Harrach, AiResearch, who supplied the program for calculation of the fluid properties and Mr. K. Bauer who constructed the apparatus. Professor H. C. Perkins, Jr. served as advisor on the project during 1975–6. Professor C. A. Sleicher of the University of Washington recommended a number of useful improvements in an earlier draft and we are grateful for them.

REFERENCES

1. K. Bammert, J. Rurik and H. Griepentrog, Highlights and future developments of closed-cycle gas turbines, ASME Paper 74-GT-7 (1974).
2. E. A. Mock, Closed Brayton cycle system optimization for undersea, terrestrial and space applications, von Kármán Institute for Fluid Dynamics, Brussels, Belgium (1970).
3. K. Bammert and R. Klein, The influence of He–Ne, He–N_2 and He–CO_2 gas mixtures on closed cycle gas turbines, ASME Paper 74-GT-124 (1974).
4. M. R. Vanco, Analytical comparison of relative heat transfer coefficients and pressure drops of inert gases and their binary mixtures, NASA TN-D-2677 (1965).
5. F. Kreith, *Principles of Heat Transfer*. International Textbook Company, Scranton (1958).
6. W. H. McAdams, *Heat Transmission*, 3rd Edn. McGraw-Hill, New York (1954).
7. J. Blom, Experimental determination of the turbulent Prandtl number in a developing temperature boundary layer, in *Proceedings of the Fourth International Heat Transfer Conference*, Vol. II, Paper FC 2.2 (1970).
8. A. Quarmby and R. Quirk, Measurements of the radial and tangential eddy diffusivities of heat and mass in turbulent flow in a plain tube, *Int. J. Heat Mass Transfer* **15**, 2309–2327 (1972).
9. A. J. Reynolds, The prediction of turbulent Prandtl and Schmidt numbers, *Int. J. Heat Mass Transfer* **18**, 1055–1069 (1975).
10. D. M. McEligot, P. E. Pickett and M. F. Taylor, Measurements of wall region turbulent Prandtl numbers in small tubes, *Int. J. Heat Mass Transfer* **19**, 799–803 (1976).
11. J. C. Hilsenrath, W. Beckett, W. S. Benedict, L. Fano, H. J. Hoge, J. F. Masi, R. L. Nuttall, Y. S. Touloukian and H. W. Wooley, NBS Circular 564 (1955).
12. W. C. Reynolds, *Thermodynamics*, 2nd Edn, p. 228. McGraw-Hill, New York (1968).
13. W. C. Reynolds and H. C. Perkins, *Engineering Thermodynamics*. McGraw-Hill, New York (1968).
14. J. O. Hirschfelder, C. F. Curtiss and R. B. Bird, *Molecular Theory of Gases and Liquids*. John Wiley, New York (1964).
15. R. A. Dawe and E. B. Smith, Viscosities of the inert gases at high temperature, *J. Chem. Phys.* **52**, 693–703 (1970).
16. A. S. Kalelkar and J. Kestin, Viscosity of He–Ar and He–Kr binary gaseous mixtures in the temperature range 25–720°C, *J. Chem. Phys.* **52**, 4248–4261 (1970).
17. V. K. Saxena and S. C. Saxena, Measurements of the thermal conductivity of helium using a hot-wire type of thermal diffusion column, *Br. J. Appl. Phys. (J. Phys. D.)* **1**, 1341–1351 (1968).
18. R. DiPippo and J. Kestin, The viscosity of seven gases up to 500°C and its statistical interpretation, in *Fourth Symposium on Thermal Physical Properties*, pp. 304–313 (1969).
19. Y. S. Touloukian and C. Y. Ho, *Thermophysical Properties of Matter*. Plenum Press, London (1970).
20. R. S. Gambhir and S. C. Saxena, Thermal conductivity of binary and ternary mixtures of krypton, argon and helium, *Molec. Phys.* **11**, 233–241 (1966).
21. H. Cheung, L. A. Bromley and C. R. Wilke, Thermal conductivity of gas mixtures, *A.I.Ch.E. Jl* **8**, 221–228 (1962).
22. J. N. Peterson, T. F. Hahn and E. W. Comings, Thermal conductivity of mixtures of argon–helium, argon–nitrogen and argon–neon, *A.I.Ch.E. Jl* **17**, 289–291 (1971).
23. E. A. Mason and H. von Ubisch, Thermal conductivity of rare gas mixtures, *Physics Fluids* **3**, 355–361 (1960).
24. J. M. Gandhi and S. C. Saxena, Correlated thermal conductivity data of rare gases and their binary mixtures at ordinary pressures, *J. Chem. Engng* **13**, 357–361 (1968).
25. D. M. McEligot, M. F. Taylor and F. Durst, Internal forced convection to mixtures of inert gases, *Int. J. Heat Mass Transfer* **20**, 475–486 (1977).
26. C. A. Bankston and D. M. McEligot, Turbulent and laminar heat transfer to gases with varying properties in the entry region of circular ducts, *Int. J. Heat Mass Transfer* **13**, 319–344 (1970).
27. E. R. van Driest, On turbulent flow near a wall, *J. Aeronaut. Sci.* **23**, 1007–1011 and 1036 (1956).
28. H. Reichardt, Complete representation of turbulent velocity distribution in smooth pipes, *Z. Angew. Math. Mech.* **31**, 208 (1951).
29. T. B. Drew, E. C. Koo and W. M. McAdams, The friction factor in clean, round pipes, *Trans. Am. Inst. Chem. Engrs* **28**, 56–72 (1932).

30. D. A. Campbell and H. C. Perkins, Variable property turbulent heat and momentum transfer for air in a vertical rounded corner triangular duct, *Int. J. Heat Mass Transfer* **11**, 1003–1012 (1968).
31. W. K. Moen, Surface temperature measurement, *Inst. Control Syst.* **33**, 70–73 (1960).
32. W. G. Hess, Thermocouple conduction error with radiation heat loss, M.S.E. Thesis, University of Arizona (1965).
33. P. E. Pickett, Heat and momentum transfer to internal, turbulent flow of helium–argon mixtures in circular tubes, M.S.E. Report, Aerospace and Mechanical Engineering Department, University of Arizona (1976).
34. S. J. Kline and F. A. McClintock, The description of uncertainties in single sample experiments, *Mech. Engng* **75**, 3–8 (1953).
35. J. A. Malina and E. M. Sparrow, Variable-property, constant-property, and entrance-region heat transfer results for turbulent flow of water and oil in a circular tube, *Chem. Engng Sci.* **19**, 953–961 (1964).
36. W. M. Kays, *Convective Heat and Mass Transfer*. McGraw-Hill, New York (1966).
37. C. A. Sleicher and M. W. Rouse, A convenient correlation for heat transfer to constant and variable property fluids in turbulent pipe flow, *Int. J. Heat Mass Transfer* **18**, 677–683 (1975).
38. M. F. Taylor, Correlation of friction coefficients for laminar and turbulent flow with ratios of surface to bulk temperature from 0.35 to 7.35, NASA TR R-267 (1967).
39. P. M. Magee and D. M. McEligot, Effect of property variation on the turbulent flow of gases in tubes: the thermal entry, *Nucl. Sci. Engng* **31**, 337–341 (1968).
40. W. C. Reynolds and T. Cebeci, Turbulence—calculation of turbulent flows, *Topics Appl. Phys.* **21**(5), 193–229 (1976).
41. B. E. Launder and D. B. Spalding, *Mathematical Models of Turbulence*. Academic Press, London (1972).
42. C. A. Sleicher, Experimental velocity and temperature profiles for air in turbulent pipe flow, *Trans. Am. Soc. Mech. Engrs* **80**, 693–704 (1958).
43. D. Coles, The law of the wall in turbulent shear flow, in 50 *Jahre Grenzschichtforschung*, Friedr. Veiweg, Braunschweig (1955).
44. P. S. Andersen, W. M. Kays and R. J. Moffat, The turbulent boundary layer on a porous flat plate: an experimental study of the fluid mechanics for adverse free-stream pressure gradients, Tech. Rpt. HMT-15, Mechanical Engineering, Stanford Univ. (1972).
45. R. J. Moffat, personal communications (12 July 1978, 7 August 1978).
46. M. R. F. Heikal and A. P. Hatton, Predictions and measurements of non-axisymmetric turbulent diffusion in an annular channel, *Int. J. Heat Mass Transfer* **21**, 841–848 (1978).
47. A. W. Serksnis, M. F. Taylor and D. M. McEligot, Heat transfer to turbulent flow of hydrogen–carbon dioxide mixtures, in *Heat Transfer* 1978, Vol. 2, pp. 163–168 (1978).
48. T. Y. Na and I. S. Nagib, Heat transfer in turbulent pipe flow based on a new mixing length model, *Appl. Sci. Res.* **28**, 302–314 (1973).
49. T. Cebeci, A model for eddy conductivity and turbulent Prandtl number, *J. Heat Transfer* **95**, 227–236 (1973).
50. E. R. Corino and R. S. Brodkey, A visual investigation of the wall region in turbulent flow, *J. Fluid Mech.* **37**, 1–30 (1969).
51. D. M. McEligot, P. M. Magee and G. Leppert, Effect of large temperature gradients on convective heat transfer: the downstream region, *J. Heat Transfer* **87**, 67–76 (1965).
52. D. M. McEligot, L. W. Ormand and H. C. Perkins, Internal low Reynolds number turbulent and transitional gas flow with heat transfer, *J. Heat Transfer* **88**, 239–245 (1966).

ECOULEMENT TURBULENT CHAUD EN CONDUITE DE MELANGES HELIUM–ARGON

Résumé—On présente les résultats d'une étude numérique et expérimentale du frottement et du transfert thermique pour un écoulement turbulent de mélanges hélium–argon dans des tubes circulaires, lisses, verticaux et chauffés électriquement. On considère des mélanges ayant des masses moléculaires entre 15,3 et 29,7; ces valeurs correspondent à des nombres de Prandtl moléculaire compris entre 0,42 et 0,49. Les nombres de Reynolds à l'entrée varient de 31 200 à 102 000, les températures maximales de paroi entre 392 et 828 K, le rapport maximal de température paroi—coeur jusqu'à 1,82 et les pressions de 4,7 à 9,7 atm. Les formules expérimentales connues, pour des gaz à nombre de Prandtl de l'ordre de 0,7 surestiment les nombres de Nusselt observés. Par comparaison des calculs numériques et des nombres de Nusselt mesurés pour des propriétés constantes, les nombres de Prandtl turbulent sont déterminés dans la région de paroi. La validité de l'utilisation de ces nombres de Prandtl ainsi déduits est examinée pour des conditions dans lesquelles les propriétés varient fortement.

BEHEIZTE TURBULENTE ROHRSTRÖMUNG VON HELIUM–ARGON–GEMISCHEN

Zusammenfassung—Es werden Ergebnisse einer numerischen und experimentellen Untersuchung von Reibungs- und Wärmeübergangsparametern der turbulenten Strömung von Helium–Argon–Gemischen in glatten, elektrisch beheizten vertikalen Rohren mit kreisförmigem Querschnitt dargestellt. Es werden Gemische mit Molekulargewichten zwischen 15,3 und 29,7 verwendet; diese Werte entsprechen den molekularen Prandtl-Zahlen von 0,42 bis 0,49. Die Einlauf-Reynolds-Zahlen reichen von 31,2 bis 102,0; die maximale Wandtemperatur von 392 bis 828 K; des Verhältnis der maximalen Wandtemperatur zur mittleren Fluid-temperatur bis 1,82 und der Druck von 4,7 bis 9,7 at. Es zeigte sich, daß gut bekannte experimentelle Korrelationen für Gase mit Prandtl-Zahlen in der Größenordnung von 0,7 für die erhaltenen Nusselt-Zahlen zu hohe Werte liefern. Durch Vergleich von numerischen Berechnungen mit bei konstanten Stoffwerten gemessenen Nusselt-Zahlen wurden turbulente Prandtl-Zahlen in Wandnähe bestimmt. Die Zulässigkeit der Verwendung dieser abgeleiteten turbulenten Prandtl-Zahlen wird für Bedingungen untersucht, unter denen sich die Stoffwerte sehr wesentlich ändern.

ТУРБУЛЕНТНОЕ ТЕЧЕНИЕ ГЕЛИЕВО-АРГОНОВЫХ СМЕСЕЙ В НАГРЕВАЕМЫХ ТРУБАХ

Аннотация — Представлены результаты теоретического и экспериментального исследования трения и теплообмена при турбулентном течении гелиево-аргоновых смесей в гладких вертикальных трубах, нагреваемых электрическим током. В экспериментах использовались смеси с молекулярными весами в пределах от 15,3 до 29,7. Этим значениям соответствовали молекулярные числа Прандтля от 0,42 до 0,49. Числа Рейнольдса на входе составляли от 31 200 до 102 000, максимальная температура стенки находилась в пределах от 392 до 828°К, максимальное отношение температуры стенки к среднеобъёмной температуре смеси — до 1,82, давление — от 4,7 до 9,7 атмосфер. Найдено, что существующие экспериментальные обобщенные зависимости, полученные при использовании числа Прандтля порядка 0,7, завышают значения числа Нуссельта, полученные в данном эксперименте. Путём сравнения результатов численного расчёта с измеренными значениями числа Нуссельта для жидкостей с постоянными свойствами определены значения турбулентного числа Прандтля в области стенки. Справедливость этих значений проверяется в условиях существенного изменения физических свойств жидкости.